Plasma Physics, Vol. 12, pp. 253 to 264. Pergamon Press 1970. Printed in Northern Ireland

MINIMUM-$\bar{B}$ STABILIZATION OF DRIFT WAVES IN A Q MACHINE

FRANCIS F. CHEN and KENNETH C. ROGERS*
Plasma Physics Laboratory, Princeton University, Princeton, N.J. 08540, U.S.A.

(*Received* 23 *June* 1969)

Abstract—A minimum-$\bar{B}$ geometry is created in a Q machine by inserting reverse-current loops into the vacuum chamber. The level of drift oscillations, both coherent and turbulent, is found to be greatly reduced when the loops are energized.

1. INTRODUCTION

AMONG the methods available for controlling drift or universal instabilities are the application of magnetic shear and the creation of a magnetic well (minimum-B). We have previously reported on the effectiveness of shear stabilization (CHEN and MOSHER, 1967; CHEN *et al.*, 1969); we now report on the effect of minimum-$\bar{B}$.

In toroidal confinement geometry, it is not possible to create a true magnetic well but only an average well, in which the curvature of the lines of force is alternately concave and convex, but is concave (stabilizing) when an average is taken along a line of force. In this case, instabilities can occur locally between regions of favorable curvature, and drift waves are suppressed only because they require long wavelengths $\lambda_\parallel$ in the direction of the field **B**. The effect of minimum-$\bar{B}$ is, then, to impose on the plasma a 'connection length' L_c between regions of favorable curvature, so that only waves with $\lambda_\parallel < 2L_c$ can exist. If L_c is sufficiently short, $\lambda_\parallel$ will be restricted to a range in which drift waves either have very slow growth rates or are damped by ion Landau damping.

We approximate the toroidal situation by using a linear Q machine with internal coils, as shown in Fig. 1. These coils carry current opposing the current in the external coils creating the uniform primary field B_0. In the neighborhood of each reverse coil the magnetic field is distorted into a minimum-$\bar{B}$ configuration; between coils the field remains uniform. The connection length L_c is then the distance between coils or between a coil and an end plate, since the conducting end plates can also hold down the oscillation amplitude. This geometry was first suggested to us by J. M. Dawson; we shall therefore call the internal coils Dawson coils or Dawson rings.

Since, as explained above, the effect of minimum-$\bar{B}$ is solely to introduce a connection length L_c, it would not matter if an L_c were imposed by some other device which would locally hold down the oscillation amplitude, such as a grid or an electrode with negative feedback. In the present experiment, there were actually two other effects besides minimum-$\bar{B}$ which tended to damp the waves in the neighborhood of the Dawson coils. One is viscous damping (ion–ion collisions), which is large in the 'bridge' region around each coil, where the plasma thickness is only about 3 ion Larmor radii, as contrasted with $12r_L$ in the uniform-field region.† The other effect is the

* Permanent address: Stevens Institute of Technology, Hoboken, New Jersey, U.S.A.

† The number of Larmor orbits in a tube of force, of course, remains constant as $|B|$ varies. However, in this case, the circular cross section has been stretched into a thin annulus with a large azimuthal dimension but a small radial dimension.

variation of $|B|$ along **B**, which, because of higher-order terms in r_L/R, causes the azimuthal drift-wave velocity to vary with $|B|$; the waves, therefore, cannot stay in phase in the neighborhood of the Dawson coil. These two effects ensure the local damping of drift waves in spite of the existence of magnetically shielded leads, which ordinarily would destroy the minimum-$\bar{B}$ properties of the coil at the azimuth of the leads.

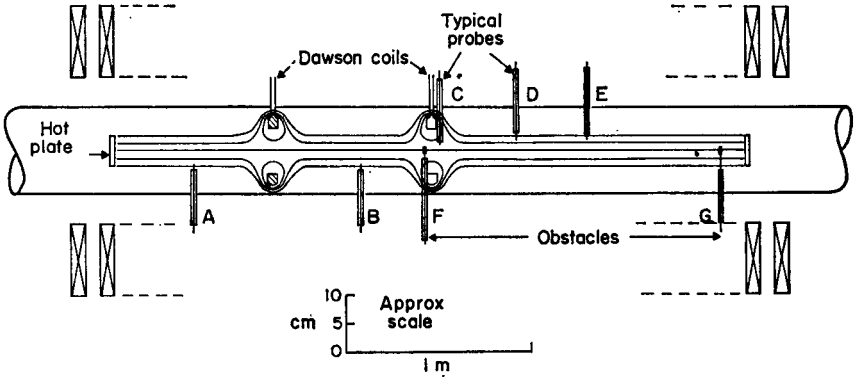

FIG. 1.—Schematic of Q machine with Dawson coils. Two coils are shown; one to three coils were used in the experiment.

2. APPARATUS

The Q machine (RYNN, 1964) produces an 0·22 eV plasma 5 cm in dia. and 326 cm long by contact ionization of potassium atoms on thermionically emitting tungsten plates. The Dawson coils consist of four turns of hollow copper conductor cast in epoxy resin. Overall dimensions are 3 in. i.d., 4·86 in. o.d., 0·7 in. thick. The outside edges are beveled to allow more room for the plasma in the bridge region. The leads are designed to be magnetically shielded with the help of an iron insert and serve also as the support. Langmuir probes are used for diagnostics.

In normal operation, B_0 is 2 kG and the Dawson coil current I_D is 22·6 kA-turns d.c. The field configuration for this case is shown in Fig. 2. The stagnation points are on the axis and 2 in. from the midplane of the coil. As I_D is reduced, the stagnation points move towards the midplane of the coil, and then upwards on the midplane towards the coil. The plasma then runs into the coil. If I_D is increased, there is more room for the plasma in the bridge region, but the water-cooling problem limits operation to pulses of $<0{\cdot}1$ sec duration. In principle, more space between the stagnation surface and the coil can be obtained by using a larger diameter coil and higher I_D; here we were limited by the power supply and by the vacuum chamber diameter.

From Fig. 2 it is seen that the length of the lines of force increases as one approaches the stagnation surface; this gives rise to a magnetic well, or a maximum in $\int \mathrm{d}l/B$. Figure 3 shows plots of $\int \mathrm{d}l/B$, the mirror ratio $R_{\mathrm{max.}}/R_{\mathrm{min.}}$ and $R_{\mathrm{max.}}$ as a function of R_0, the radial position of the line of force in the uniform-field region far from the coil. From Fig. 2 one sees that the field lines return to their undisturbed positions within a few cm of the coil.

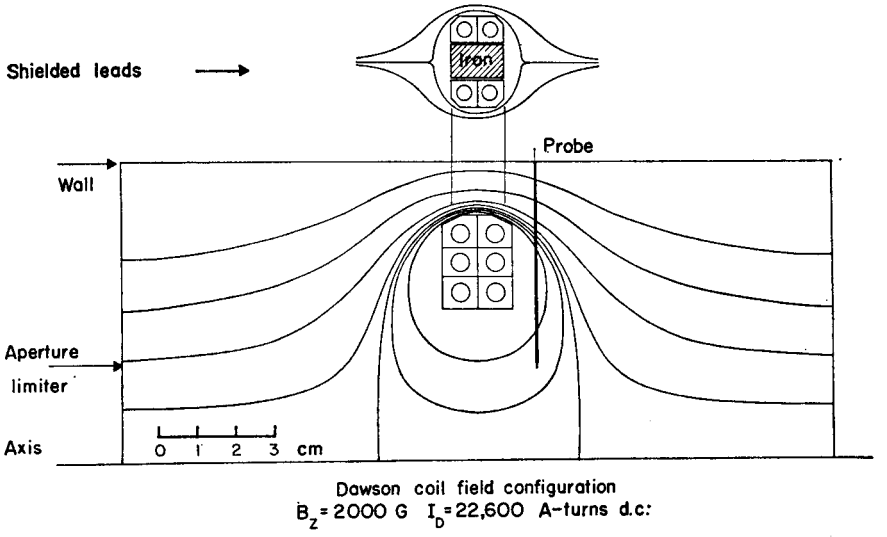

FIG. 2.—Field-line configuration around Dawson coil in normal operation. The upper inset is a 90°-rotated view showing the field lines around the magnetically shielded leads. The radius of the aperture limiter is shown. Although six turns are shown on the coil, only four of these positions are occupied; the others are crossovers.

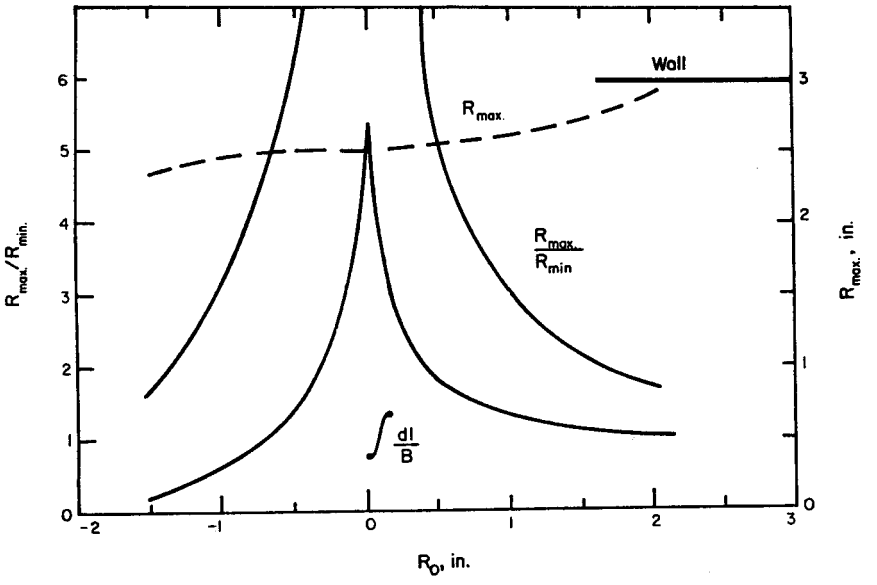

FIG. 3.—Plots of $\int dl/B$ (arbitrary units), $R_{max.}/R_{min.}$, and $R_{max.}$ as a function of R_0. Negative values of R_0 refer to closed lines surrounding the coil.

3. EFFECT OF DAWSON COILS ON DENSITY PROFILES

(a) *Flow of plasma around coils*

Before proceeding with observations of the oscillations, we checked the plasma profiles to see if the Dawson coils were operating properly. Figure 4(a) shows the density profiles near the coil, taken with the probe shown in Fig. 2 (also shown as

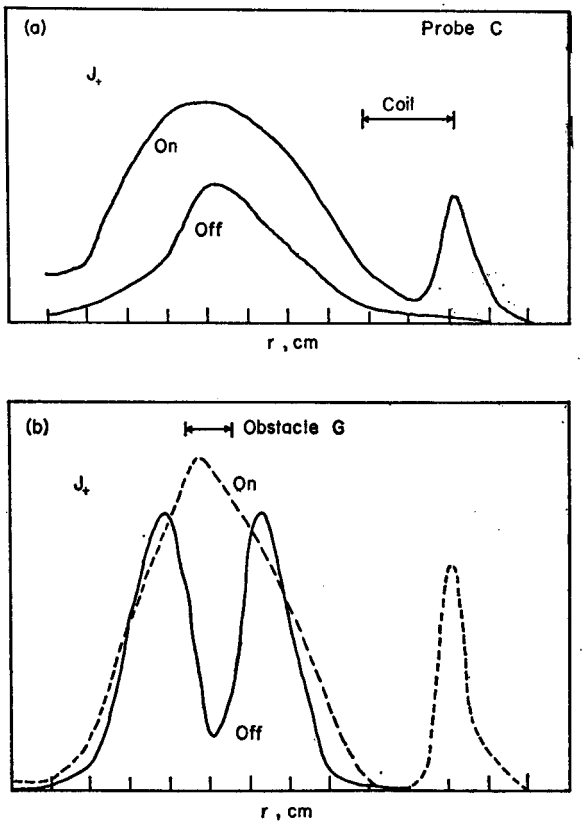

FIG. 4.—Radial profiles of density (saturation ion current to a probe) near a Dawson coil with the coil on and off. Single-ended operation, with only the right-hand hot plate (Fig. 1) in use. Probe *C* (Fig. 1) was used. (a) with no obstacle; (b) with obstacle *G* (Fig. 1) inserted on axis.

probe *C* in Fig. 1). When the coil is on, the plasma is diverted to the bridge region, and a peak appears in the proper position there. However, the density on the axis remains surprisingly high, and we made an effort to determine the origin of this central density. To eliminate the possibility that ions injected near the axis were not following the lines of force around the coil, we inserted an obstacle (*G* in Fig. 1), an 0·5 in. dia. disc, on the axis. The density profile [Fig. 4(b)] then showed a hole in the middle, as expected. However, when the coil was energized, the hole was filled, indicating that ions injected at large radii were able to migrate to the axis. The same effect was observed with the probe collecting electrons rather than ions. This cross-field transport was apparently not caused by oscillations; the oscillation level with the coil on was unmeasurably small, less than 1 per cent. The particles near the axis, as

seen by probe C, move on lines of force encircling the coil. If these particles are well trapped, a small cross-field diffusion rate could explain the observed population of these orbits. To eliminate this possibility, we inserted obstacle F (Fig. 1) to intercept particles on these orbits. This made no difference. Apparently, plasma migrates rapidly across the line of force to reach the axis without oscillations.

Figure 5 shows the effect of varying I_D to change the stagnation point location in single-ended geometry. The trapped particles in closed orbits, if any, have been

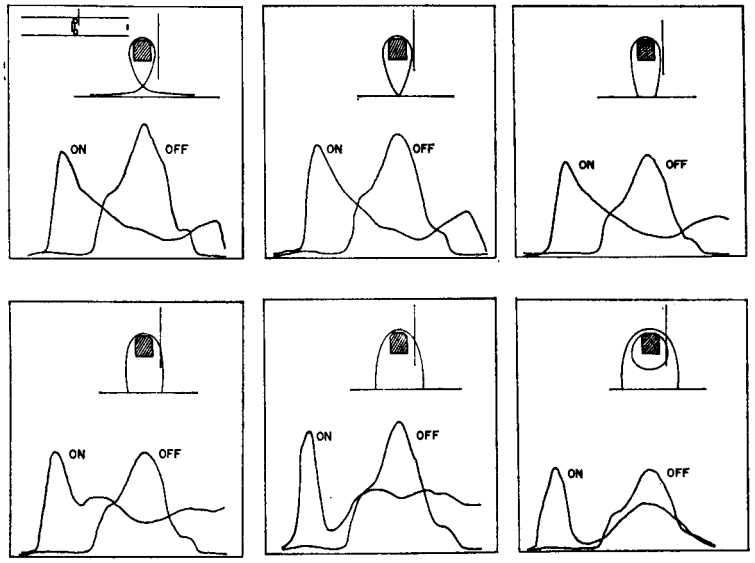

FIG. 5.—Density profiles with the Dawson coil on and off, as a function of coil current. The shape of the stagnation surface is shown in each case. The last case is the normal operating condition. The position of the probe is shown. The peak with coil 'off' corresponds to the axis; the left peak with coil 'on' corresponds to the position of the 'bridge' near the outer radius of the coil. The inset at upper left shows the machine configuration: a plug has been inserted into the coil to eliminate trapped particles in orbits encircling the coil.

eliminated by a large obstacle. For small I_D, it is seen that most particles reach the bridge region, forming a broad density peak there. The axial density is low because lines of force near the axis intersect the coil, and plasma on these lines is lost to the coil. As I_D is increased, the outside peak narrows, and the axial density rises as the stagnation surface is pushed away from the surface of the coil. A minimum occurs between these two peaks as the probe crosses lines of force which intersect the coil. From these studies, we conclude that *collisional diffusion* (mostly ion–ion collisions), or possibly convection in d.c. electric fields, *causes a rapid transport of plasma across* **B** *in the bridge region.* This is the only picture consistent with the rapid influx of plasma into the magnetic surfaces crossing the axis.

(b) *Density profiles away from coils*

We next investigated the density profiles in the uniform-field regions far from the coils. Figure 6 shows the profiles in single-ended operation, with the plasma flowing from the righthand plate in Fig. 1. It is seen that the density increases by about a factor of 2 when the Dawson coil is energized. This is easily explained by the reflection

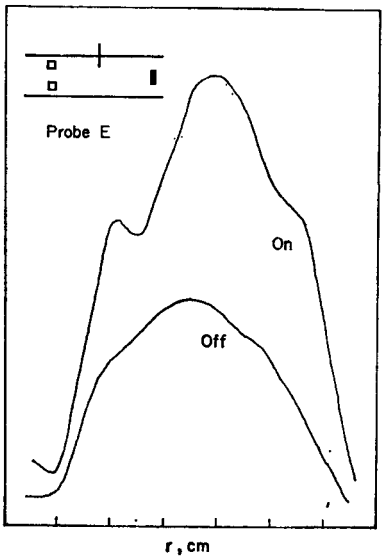

FIG. 6.—Density profiles taken with probe *E* in single-ended operation, with Dawson coil on and off.

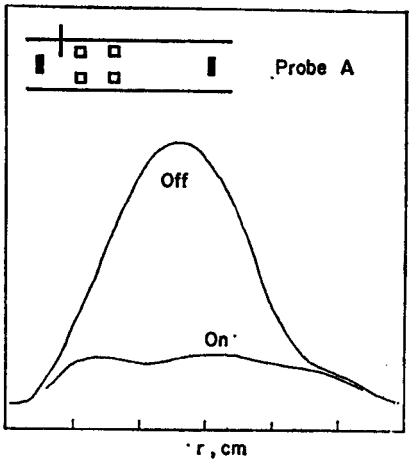

FIG. 7.—Density profiles taken with proble *A* in double-ended operation, with Dawson coils on and off. The densities are much higher than in Fig. 6.

of plasma at the strong magnetic mirror at the coil (see Fig. 3). Figure 7 shows the profiles in double-ended operation in the region between the hot plate and the first coil. The density is greatly reduced when the coil is energized; apparently, the good confinement of double-ended operation has been destroyed. The density profile is also greatly broadened; this is consistent with our deduction that large collisional diffusion occurs in the bridge region. Figure 8 shows the profiles in the region between two Dawson coils. Here turning the coils on makes the density even lower and the profile even broader, because the only particles that can reach this region are those that can penetrate the magnetic mirrors at the coils.

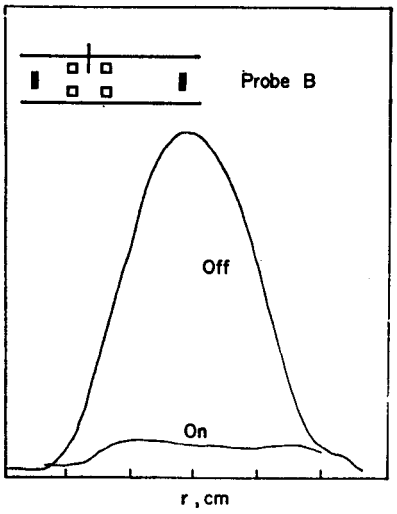

FIG. 8.—Density profiles taken with probe B in double-ended operation, with Dawson coils on and off.

(c) *Causes of loss of confinement*

The large decrease in density seen in Fig. 7 indicates that the plasma confinement time has been shortened by the Dawson coils. Typically, the peak density n_p is reduced by a factor of 5·5, and the average density by a factor 2·5. If the confinement time τ is defined by

$$\Phi_i \tau = 2\pi \int nr \, dr \, dz,$$

where Φ_i is the ion input flux from the end plates, then τ typically falls from 10 msec to 2·3 msec when the coils are turned on. This applies to the geometry of Fig. 7, where the plasma length is reduced by a factor of 4·5 and Φ_i by a factor of 2 when the coil is energized (flux from the far end plate is negligible).

We have determined that the increased losses are caused by two effects of approximately equal magnitude: increased convection due to stray magnetic fields from the return leads, and collisional diffusion (or convection) to the Dawson coil in the bridge region. To test the effect of the return leads, we reversed the current in the Dawson coils, so that the loss to the coils should be eliminated. The plasma profile was then not broadened, but the density between coils still dropped by about a factor of 3. When the return leads were moved farther away from the plasma, the density did not change when the coils were energized in the reversed direction but fell by about a factor of 3 when I_D was in the normal direction.

To test for losses to the coils, we coated one coil with copper and measured the change in current collected on the coating when the coil was turned on. The result was consistent with the picture that collisional diffusion to the coil in the bridge region caused the remainder of the losses. These losses increased when a large negative potential was applied to the coil coating and decreased when the Larmor radius was decreased by pulsing to larger I_D, keeping I_D/B_0 constant. The change in plasma lifetime caused by these losses will affect the interpretation of the data.

4. STABILIZATION OF SINGLE MODES

(a) *Double-ended operation*

By working near the threshold of excitation, one can observe the stabilization of a sinusoidal oscillation which can be identified as a resistive drift wave by well-established techniques (HENDEL *et al.*, 1968). Figure 9 shows a 3·4 kHz oscillation on two probes 90° apart in azimuth. By rotating one of the probes in azimuth, we determined that this was an $m = 2$ mode traveling in the direction of the ion diamagnetic drift v_{di}. Figure 10 shows the maximum oscillation amplitude n_1/n_0 measured with probes at various axial positions; this shows a standing wave with $k_\parallel = \pi/L$. Figure 11 shows

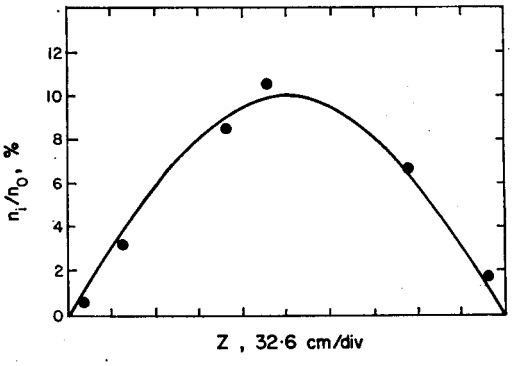

FIG. 10.—Oscillation amplitude n_1/n_0 vs. axial position for the wave of Fig. 9. The hot plates are at the extreme left and right. The line represents the ideal cosine distribution for a standing wave with nulls at the plates.

the potential distribution in the plasma and the oscillation amplitude profile, with the Dawson coils off. Figure 12 shows the density profiles with the Dawson coils on and off. From these profiles, one can compute the theoretical drift-wave frequency. This turns out to vary with radius, but we can make a rough estimate by measuring the gradients at the radius of maximum oscillation amplitude. From the density gradient, we obtain $\omega^* \equiv -(m/r)(KT/eB)(n_0'/n_0) = 20{\cdot}5$ kHz. We have included the effect of viscosity, which amounted to an 8 per cent correction. From the gradient of potential, we obtain $\omega_E \equiv -(m/r)(E_r/B) = -28{\cdot}0$ kHz, where the minus sign indicates a rotation in the direction of v_{di}. From the observed frequency $\omega = -21{\cdot}4$ kHz, we then obtain $\omega - \omega_E = 0{\cdot}32\omega^*$ for the frequency in the $E = 0$ frame. This frequency is somewhat smaller than expected of drift waves; but since it is the difference of two large numbers, the inaccuracy of our local approximation can easily account for the discrepancy.

We therefore have a drift wave of the type studied extensively by HENDEL *et al.* (1968). The stabilization of this wave is shown in Fig. 13. At the position of maximum initial wave amplitude, turning the Dawson coils on reduces the amplitude by more than a factor of 100. The stabilization is observed at all radii. It is also observed at all axial positions: we have measured the profiles and the stabilization ratio with probes *A*, *B*, *D*, *E* and *F* (Fig. 1). Changing the potential on the aperture limiter has no effect on the stabilization of the wave.

A glance at Fig. 12, however, shows that energizing the Dawson coils changes more than just the connection length. The density gradient, the collision frequency,

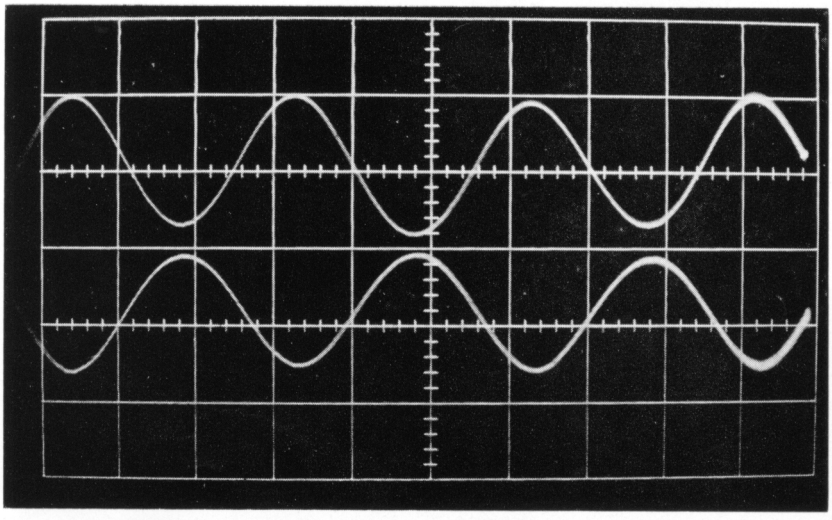

FIG. 9.—Saturation ion current on two probes displaced 90° in azimuth. AC coupled. Sweep speed: 100 μsec/cm, right to left. Dawson coil off. Probe D (Fig. 1) at position of maximum oscillation amplitude. $B = 1{\cdot}97$ kG.

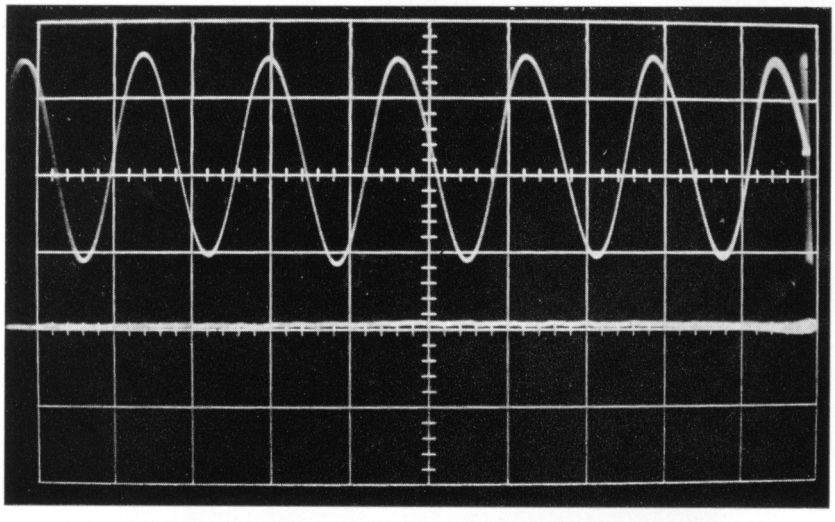

FIG. 13.—Ion current oscillations on probe D with the Dawson coils off (top trace) and on (bottom trace). Sweep speed: 200 μsec/cm, right to left. AC coupled; same gain on both traces.

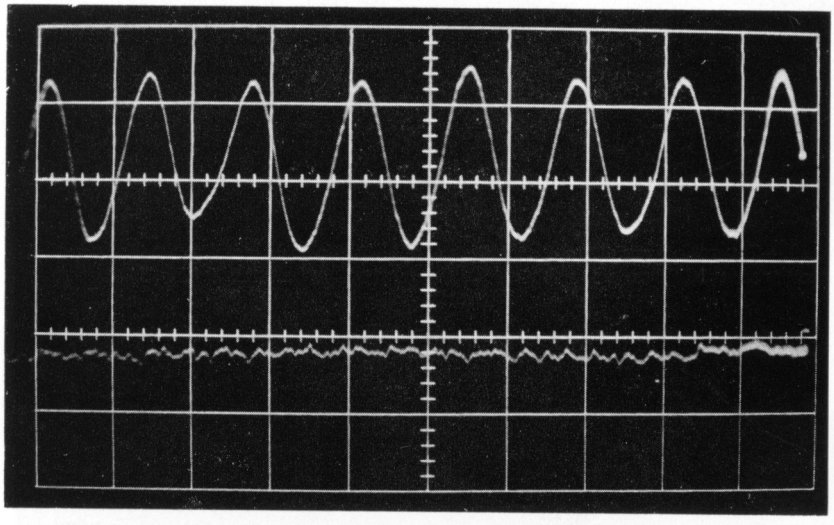

FIG. 15.—Stabilization of oscillations in single-ended operation. Caption of Fig. 13 applies.

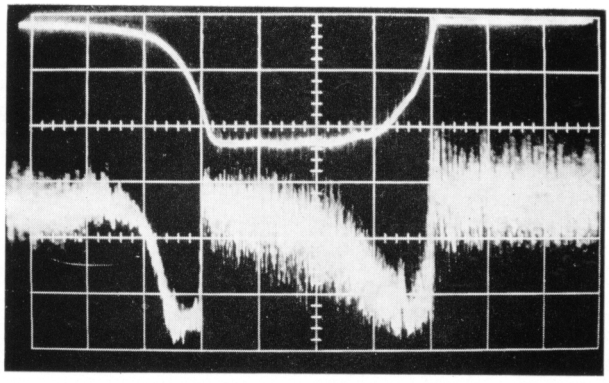

(a)

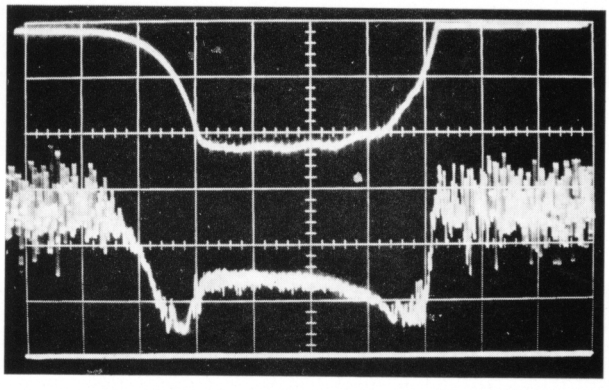

(b)

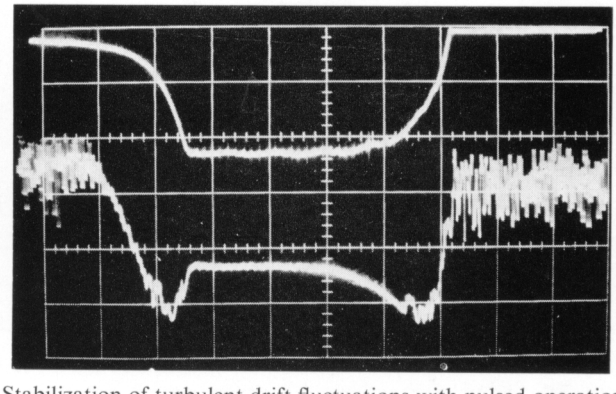

(c)

FIG. 16.—Stabilization of turbulent drift fluctuations with pulsed operation of Dawson coils. Top trace: Dawson coil current, 20 kA-turns/cm, increasing downwards. Bottom trace: probe current, dc coupled, with baseline at bottom of grid. Sweep speed: 20 msec/cm, right to left. (a), (b) and (c) refer to the probe positions shown in Fig. 17. The gain has been increased 4 times in (a).

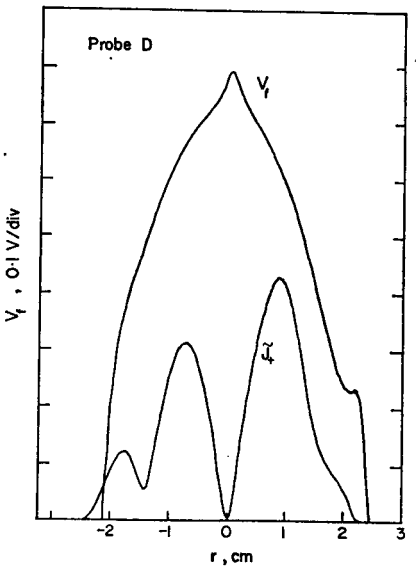

FIG. 11.—Radial profiles of probe floating potential V_f and oscillation amplitude $\tilde{J}_+$ (arbitrary units) for the oscillation of Fig. 9.

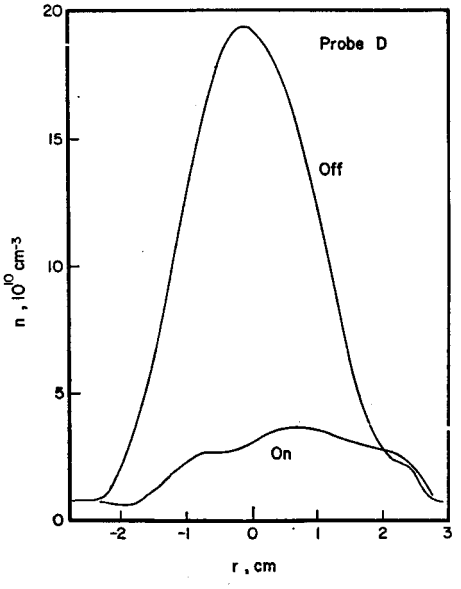

FIG. 12.—Density profiles with the Dawson coils off (same conditions as in Figs. 9–11) and with the coils on.

the radial electric field, and the plasma lifetime do not remain constant when the coils are turned on. Near threshold, a small change in any of these quantities can greatly affect the wave. From these data, we cannot tell which mechanism is responsible for the stabilization. We can state, however, that the Dawson coils *always* reduce the wave amplitude to the noise level and never have the opposite effect.

(b) *Single-ended operation*

To eliminate the possibility that the oscillations are suppressed only because the plasma lifetime τ is decreased, we operated single-ended, with one of the hot plates

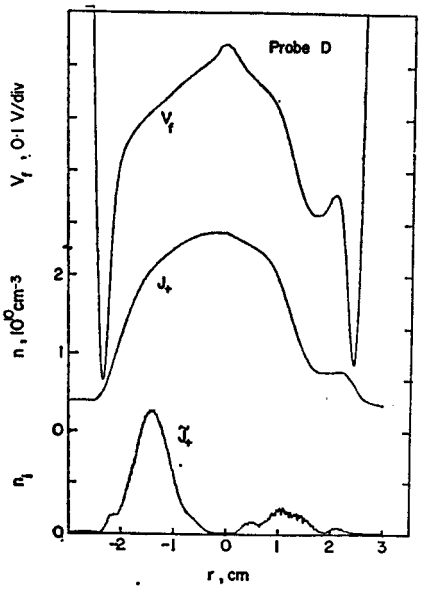

FIG. 14.—x-y recorder traces of radial profiles of floating potential V_f, ion current J_+, and ion current oscillation amplitude $\tilde{J}_+$ (arbitrary units) at probe D in single-ended operation.

masked off by a negatively biased cold plate. In this case, ions are collected at the cold plate after only one pass down the machine: and τ is so short that the Dawson coil cannot make it shorter. In fact, as explained in Section 3(b), the magnetic mirror at the coil causes the density to increase with the coils on. The density profiles at probe E are shown in Fig. 6. The corresponding profiles at probe D are shown in Fig. 14. In single-ended operation, the longitudinal streaming of the plasma, the asymmetric profiles, and the complicated boundary condition at the cold plate make it difficult to identify a drift wave with certainty. Nevertheless, we appeared to have an $m = 5$ mode with $f = 3{\cdot}7$ kHz and $n_1/n_0 = 0{\cdot}08$ at $B = 2$ kG and $n_p = 2{\cdot}5 \times 10^{10}$ cm^{-3}. The stabilization of this mode by the Dawson coils is shown in Fig. 15. It is seen that the oscillation has been reduced to the level of the amplifier noise, in spite of the fact that the density has increased rather than decreased, as in the double-ended case.

5. STABILIZATION OF TURBULENT FLUCTUATIONS

Near threshold, small perturbations of the equilibrium conditions can put the plasma into a stable regime. To test stabilization far from threshold, we increased B_0 to 3240 G and I_D to 44 kA-turns by operating in 80-msec pulses. The drift oscillations were turbulent under these conditions, and the effect of the Dawson coils on

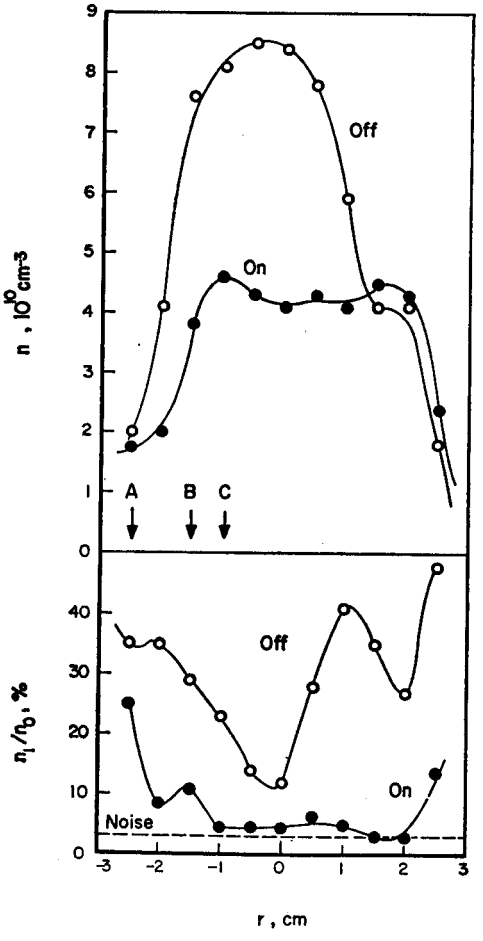

FIG. 17.—Density and oscillation amplitude profiles with the Dawson coils off and on, for the conditions of Fig. 16. Probe *D*.

them is shown in Fig. 16. From pictures such as these, we measured the effect of the minimum-$\bar{B}$ geometry on the average density and on the oscillation amplitude ($n_1 \equiv \frac{1}{2}\tilde{n}_{\text{peak-to-peak}}$). The results are shown in Fig. 17. We note the following: (1) The decrease in peak density is only a factor of 2 because at the high field the diffusive loss to the coil is less than in Section 4. The plasma lifetime, therefore, has not been greatly decreased by pulsing the coils. (2) At position A, the oscillations are high-frequency 'edge' oscillations (KENT *et al.*, 1969); these are not greatly affected by the minimum-$\bar{B}$ geometry. (3) At position *C*, the oscillations are suppressed by a large factor; however, this is due to the broadening of the density profile so that $\nabla n_0 \approx 0$

at position C when the coils are on. (4) At position B, $\nabla n_0/n_0$ is large in both cases (coils on and off), but there is still a sizable reduction in the oscillation amplitude. Similar results have been obtained also with probe B, in the section between two coils, and at higher densities, when n_1/n_0 is smaller to begin with.

6. SUMMARY

We have shown that the drift-wave amplitude is greatly reduced by a minimum-$\bar{B}$ field both near threshold and far from threshold. No detailed comparison with theory regarding the dependence on connection length was possible because the Dawson coils introduced spurious effects, such as a decrease in plasma lifetime and a broadening of the density profile. However, even when these two effects were removed, stabilization was still observed. Unfortunately, loss of plasma to the coils prevented us from observing a rise in density when the oscillations were stabilized.

Acknowledgments—We are grateful to K. WAKEFIELD, P. BONANOS, H. JOHNSON and R. WINTRISS for the design and construction of the Dawson coils, and to K. P. MANN for operating the machine under difficult conditions. We thank Dr. J. M. DAWSON for suggesting the experiment, but we hope that the next suggestion will be easier to carry out.

This work was performed under the auspices of the U.S. Atomic Energy Commission, Contract AT(30-1)-1238.

REFERENCES

CHEN F. F. and MOSHER D. (1967) *Phys. Rev. Lett.* **18**, 639.

CHEN F. F., MOSHER D. and ROGERS K. C. (1969) *Plasma Phys. and Controlled Nucl. Fusion Res.*, Vol. 1, p. 625. International Atomic Energy Agency, Vienna.

HENDEL H. W., CHU T. K. and POLITZER P. A. (1968) *Physics Fluids* **11**, 2426.

KENT G., JEN N. and CHEN F. F. (1969) *Physics Fluids* **12**, 2140.

RYNN N. (1964) *Rev. scient. Instrum.* **35**, 40.